Journal Pre-proof

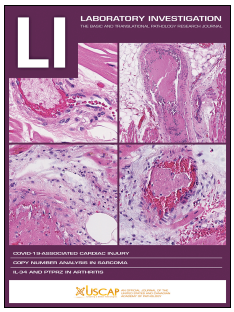

Genome-wide SNP-based Profiling of Loss of Heterozygosity Reveals Distinct Molecular Subgroup–specific Patterns in Gastrointestinal Stromal Tumors (GIST)

Thais Maloberti, Margherita Nannini, Annalisa Astolfi, Maria Concetta Nigro, Livia Gozzellino, Alice Costa, Maria Giulia Pirini, Antonio De Leo, Marco Grillini, Bruno Vincenzi, Elena Fumagalli, Antonella Brunello, Giovanni Grignani, Sandra Aliberti, Angela Dalia Ricci, Fabio Gelsomino, Giovanni Tallini, Maria Abbondanza Pantaleo, Dario de Biase

PII: S0023-6837(26)00078-4

DOI: https://doi.org/10.1016/j.labinv.2026.106148

Reference: LABINV 106148

To appear in: *Laboratory Investigation*

Received Date: 9 March 2026

Revised Date: 25 May 2026

Accepted Date: 16 June 2026

Please cite this article as: Maloberti T, Nannini M, Astolfi A, Nigro MC, Gozzellino L, Costa A, Pirini MG, De Leo A, Grillini M, Vincenzi B, Fumagalli E, Brunello A, Grignani G, Aliberti S, Ricci AD, Gelsomino F, Tallini G, Pantaleo MA, de Biase D, Genome-wide SNP-based Profiling of Loss of Heterozygosity Reveals Distinct Molecular Subgroup–specific Patterns in Gastrointestinal Stromal Tumors (GIST), *Laboratory Investigation* (2026), doi: https://doi.org/10.1016/j.labinv.2026.106148.

Genome-wide SNP-based Profiling of Loss of Heterozygosity Reveals Distinct Molecular Subgroup–specific Patterns in Gastrointestinal Stromal Tumors (GIST)

Thais Maloberti[1]*, Margherita Nannini[2,3]*, Annalisa Astolfi[2,4], Maria Concetta Nigro[2], Livia Gozzellino[2], Alice Costa[4], Maria Giulia Pirini[5], Antonio De Leo[1,2], Marco Grillini[5], Bruno Vincenzi[6], Elena Fumagalli[7], Antonella Brunello[8], Giovanni Grignani[9], Sandra Aliberti[9], Angela Dalia Ricci[10], Fabio Gelsomino[11], Giovanni Tallini[1,2], Maria Abbondanza Pantaleo[2,3]** & Dario de Biase[1,12]**

[1] Solid Tumor Molecular Pathology Laboratory, IRCCS Azienda Ospedaliero Universitaria di Bologna, Bologna, Italy
[2] Department of Medical and Surgical Sciences (DIMEC), University of Bologna, Bologna, Italy
[3] Medical Oncology, IRCCS Azienda Ospedaliero-Universitaria di Bologna, Bologna, Italy
[4] IRCCS Azienda Ospedaliero-Universitaria di Bologna, Bologna, Italy
[5] Pathology Unit, IRCCS Azienda Ospedaliero-Universitaria di Bologna, Bologna, Italy
[6] Department of Medical Oncology, Campus Biomedico University of Rome, Rome, Italy
[7] Medical Oncology Unit 2, Fondazione IRCCS, Istituto Nazionale dei Tumori, Milano, Italy
[8] Department of Oncology, Medical Oncology 1, Veneto Institute of Oncology IOV - IRCCS, Padua, Italy
[9] Candiolo Cancer Institute, FPO – IRCCS, Candiolo, Italy
[10] Medical Oncology Unit, National Institute of Gastroenterology, IRCCS "S. de Bellis" Research Hospital, Castellana Grotte, Italy.
[11] Department of Oncology and Hematology, Division of Oncology, University Hospital of Modena, Modena, Italy
[12] Department of Pharmacy and Biotechnology (FaBit), University of Bologna, Bologna, Italy

* Equal first contribution
** Equal last contribution

Corresponding author: Annalisa Astolfi annalisa.astolfi@unibo.it

Abstract

Purpose: Gastrointestinal stromal tumors (GIST) are molecularly heterogeneous neoplasms defined by mutually exclusive driver alterations (*KIT*, *PDGFRA*, *SDH*, *BRAF*, *RAS* and *NF1*). However, driver mutations alone do not fully explain their biological and clinical variability. Chromosomal imbalances and loss of heterozygosity (LOH) may represent an additional layer of tumor characterization. We developed a single-nucleotide polymorphism (SNP)-based next-generation sequencing (NGS) panel enabling genome-wide LOH assessment from formalin-fixed paraffin-embedded tissue.

Materials and Methods: Forty-nine GIST cases molecularly classified by targeted NGS (*KIT* n=19, *PDGFRA* n=9, SDH-*deficient* n=8, *NF1* n=7, quadruple wild type [qWT] n=6) were analyzed. LOH was inferred from variant allele frequency patterns across 1,826 genome-wide SNPs.

Results: Chromosome 14 was the most commonly affected (63%), followed by chromosomes 22 (45%), 15 (41%), 21 (27%), and 13 (20%). Loss of chromosome arm 1p occurred in 43% of tumors. Distinct subgroup-specific patterns emerged: KIT-mutant GIST exhibited the highest degree of genomic instability, whereas both SDH-*deficient* tumors and *PDGFRA*-mutant GIST displayed minimal chromosomal instability. NF1-mutant tumors showed recurrent single-arm chromosome 17 LOH. qWT GISTs were heterogeneous, including one case with extensive chromosomal instability.

Conclusions: Genome-wide SNP-based LOH profiling reveals distinct, subgroup-specific patterns of chromosomal imbalance in GIST and may serve as a feasible complementary approach to driver mutation analysis for refined molecular characterization and potential future clinical utility.

Keywords: GIST, LOH, NGS, SNPs

Introduction

Gastrointestinal stromal tumors (GIST) are rare mesenchymal neoplasms of the gastrointestinal tract, most commonly arising in the stomach and small intestine. From a molecular standpoint, GISTs are characterized by mutually exclusive oncogenic alterations involving *KIT, PDGFRA*, the succinate dehydrogenase (*SDH*) complex (through either mutations or methylation), *BRAF*, *RAS,* and *NF1*, which define biologically and clinically distinct subgroups[1]. Less than 5% of GISTs do not harbor alterations in any of the genes mentioned above, referred to as quadruple wild-type (qWT) GIST[2-4]. Molecular classification is therefore essential for diagnostic accuracy, prognostic stratification, and therapeutic decision-making.

Despite the central role of these driver alterations, they do not fully explain the biological heterogeneity observed among GISTs. Accumulating evidence indicates that additional genomic events, particularly chromosomal imbalances and loss of heterozygosity (LOH), contribute to tumor development and progression[5-9]. Recurrent losses involving chromosome arms 1p, 14q, and 22q have been consistently reported and are thought to harbor genes relevant to cell cycle control, DNA repair, and tumor suppression[5-9].

LOH represents a critical mechanism of genomic instability, especially when it affects tumor suppressor genes. Its clinical relevance has been well established in several tumor types, where specific LOH patterns have diagnostic, prognostic, or therapeutic implications[10]. In adult gliomas, LOH in both the p arm of chromosome 1 and the q arm of chromosome 19 is diagnostic for oligodendroglioma[11], whereas in neuroblastoma, loss of 1p, loss of 11q, and gain of 17q are negative predictors for long-term overall survival[12]. In ovarian cancer, LOH is particularly relevant from a therapeutic perspective, as it is one of the parameters used to assess genomic instability and homologous recombination deficiency (HRD) status, which are essential for determining eligibility for PARP inhibitor therapy[13].

In GIST, however, LOH has historically been investigated using locus-specific assays or low-resolution genome-wide approaches, such as comparative genomic hybridization or targeted arrays[5-7]. While these studies have established the relevance of chromosomal imbalances in GIST biology, they have limited resolution and scalability, and do not allow comprehensive, uniform, and genome-wide assessment of allelic imbalance across different molecular subgroups.

To address these limitations, we developed a novel single-nucleotide polymorphism (SNP)-based next-generation sequencing (NGS) panel specifically designed for genome-wide detection of LOH. By applying this approach to a molecularly heterogeneous cohort, we aimed to characterize LOH patterns across distinct GIST molecular subgroups and to explore whether subgroup-specific LOH signatures could provide additional insights into GIST biology.

Material and Methods

Patients

A total of 50 formalin-fixed and paraffin-embedded (FFPE) GIST samples, previously analyzed via NGS multi-gene panel at the Solid Tumor Molecular Pathology Laboratory of IRCCS Azienda Ospedaliero-Universitaria of Bologna (Italy)[14], were further characterized for this study. All pathological, clinical, and follow-up data were anonymously collected from in- and out-patient medical records in an electronic database.

Confirmed written consent for molecular testing was obtained from all patients. The study was performed in accordance with the Declaration of Helsinki protocols. The study was reviewed and approved by the local Institutional Ethical Committee of Azienda Ospedaliero-Universitaria Policlinico S. Orsola-Malpighi, Bologna, Italy (approval number 113/2008/U/Tess).

Molecular analysis

DNA was extracted from 2-3 10 µm unstained thick sections, based on a pathologist's selection on the last hematoxylin and eosin slide (H&E). DNA was quantified using a Qubit fluorometer (Thermo Fisher Scientific, Waltham, MA, USA) and first analyzed with two lab-developed multigene-NGS panels designed to investigate common hot-spot mutations in GIST[12]. In order to evaluate the presence of LOH, a SNP-NGS panel was designed to investigate 1826

SNPs scattered throughout the genome, involving all chromosomes. The analysis for both panels was performed using the Gene Studio S5 Prime sequencer (Thermo Fisher Scientific). SNP-based NGS panel allows the detection of LOH across individual chromosomes by analyzing the variant allele frequency (VAF) of each SNP, as LOH leads to characteristic shifts in allele frequencies that can be assessed using SNPs distributed throughout the genome. The VAF of heterozygous SNPs is typically around 50%, while homozygous SNPs approach 100%; in the presence of LOH, SNPs deviate from these expected values, resulting in a detectable allelic imbalance.

SNP imbalance was defined as the following percentage of mutation: $10\% \leq SNP \leq 40\%$ or $60\% \geq SNP \geq 90\%$. SNPs with a percentage <10% or >90% were considered non-informative[9]. Total chromosomal imbalance occurs when almost all informative SNPs present LOH throughout the entire chromosome. SNPs distribution across the genome was analyzed using a custom-developed tool performed by Perl (version 5.30.1) (Figure 1). For the analysis of methylation status of *SDHC* genes, genomic DNA was treated with bisulfite using the EZ DNA Methylation Kit (Zymo Research, Irvine, CA), following manufacturer's instructions.

Primers for amplification of bisulfite-modified DNA were designed on CpG27 of *SDHC* (chr1:161284119-161284451)[15]. Amplicons were then purified and sequenced on both strands using

the Big Dye Terminator v1.1 cycle sequencing kit (Life Technologies) on the ABI 3730 Genetic Analyzer (Applied Biosystems, Monza, Italy).

Based on NGS analysis and the methylation status of the *SDHC* gene, samples were stratified into the following molecular subgroups: *KIT*-mutant GIST, *PDGFRA*-mutant GIST, *SDH*-deficient GIST, and *NF1*-mutant GIST. The remaining samples that did not exhibit any alterations were classified as qWT GIST. Statistical analyses were performed using the GraphPad Prism tool (v.10). The different groups were compared for the distribution of the number of chromosomes affected by loss of heterozygosity (LOH) using the Kruskal–Wallis non-parametric test.

Results

Patients' cohort

A total of 50 GIST cases were included in the study; one sample was excluded due to insufficient DNA quality for LOH analysis. The remaining 49 cases were successfully analyzed. The main clinicopathological characteristics of the cohort are summarized in Table 1. According to molecular classification, 19 (39%) were *KIT*-mutant GIST, 9 (18%) *PDGFRA*-mutant GIST, 8 (16%) SDH-*deficient* GIST, 7 (14%) *NF1*-mutant GIST, and 6 (12%) qWT GIST.

KIT-mutant GIST showed a nearly equal sex distribution and were most frequently located in the ileum, followed by the stomach. Forty-two percent of cases were classified as high risk according to the Miettinen criteria, and the only two cases presenting with advanced disease at diagnosis belonged to this subgroup. In contrast, *PDGFRA*-mutant GISTs were exclusively gastric and all localized at the time of diagnosis. SDH-*deficient* GIST predominantly affected female patients (62%), showed exclusive gastric localization, and were more frequently classified as high risk. *NF1*-mutant GIST also predominantly affected females, displayed exclusive localization in the small intestine, and were evenly distributed across risk classes. Finally, qWT-GIST predominantly affected males (83%), were most frequently located in the ileum, and exhibited a relatively even distribution across risk categories.

Genome-wide LOH analysis

Genome-wide LOH analysis revealed heterogeneous chromosomal involvement across the cohort. The chromosomes most frequently affected by LOH were chromosome 14 (63% of cases), followed by chromosomes 22 (45%), 15 (41%), 21 (27%), and 13 (20%). All other chromosomes exhibited LOH in less than 20% of cases.

When considering LOH events restricted to individual chromosome arms, loss of chromosome arm 1p was the most frequent alteration, detected in 43% of cases, whereas loss of other chromosome

arms occurred at frequencies below 10%. A detailed summary of LOH frequency by chromosome and molecular subgroup is provided in Supplementary Table S1.

Stratification by molecular subgroup revealed marked heterogeneity in LOH patterns, with distinct profiles emerging for each subgroup (Figure 2).

In particular, *KIT*-mutant GIST exhibited the highest overall burden of chromosomal LOH: there are an average of 5 altered chromosomes per case (Figure 3). Only chromosomes 1, 17, and 19 showed no detectable alterations on the entire chromosome, while chromosome 22 was affected in 79% of cases and chromosome 14 in 74%. LOH involving chromosome arm 1p was observed in 63% of *KIT*-mutant GIST cases. *PDGFRA*-mutant GIST showed LOH affecting chromosomes commonly altered in *KIT*-mutant GIST, but at a markedly lower frequency (average of 1,5 altered chromosomes per case), consistent with greater cytogenetic stability of this molecular subgroup (Figure 3). LOH was detected in only five chromosomes, with chromosome 14 being the most frequently affected (78%). SDH-*deficient* GIST displayed the most stable genomic profile, with LOH limited to only three chromosomes and an average of 0.5 altered chromosomes per case. Among these, chromosome 13 was the most frequently altered, occurring in 25% of cases (Figure 3). In NF1-mutant GIST, LOH was frequently observed on chromosome 14 (86% of cases), followed by chromosome 15 (57%). Notably, LOH involving chromosome 17 was detected in 86% of cases, affecting either the p or the q arm in a mutually exclusive manner. No LOH events were observed in the remaining chromosomes.

qWT GIST showed marked heterogeneity: five of six cases (83%) exhibited LOH involving three or fewer chromosomes, whereas one case demonstrated extensive chromosomal instability, with LOH affecting 18 chromosomes (Figure 3). Within this subgroup, the most frequently altered chromosomes were chromosome 22 (50%), followed by chromosomes 13 (33%) and 14 (50%). LOH involving chromosome arm 1p was detected in only one case, like chromosome arms 16q, 19q, and 20q.

Discussion

GISTs are characterized by a heterogeneous genomic landscape. Although the majority of cases harbor activating alterations in key driver genes such as *KIT*, *PDGFRA*, *SDH*, *BRAF*, *RAS,* or *NF1*, these canonical events alone do not fully account for the biological diversity and clinical behavior observed across GIST. Increasing evidence indicates that additional mechanisms of genomic instability, including chromosomal imbalances and LOH, play a relevant role in GIST pathogenesis and progression, this has already been demonstrated by previous cytogenetic studies[5-7,16,17].

In this study, we developed and applied a novel SNP-based next-generation sequencing panel specifically designed for genome-wide LOH detection using routine FFPE samples. This approach

enabled a comprehensive assessment of chromosomal LOH patterns across a molecularly heterogeneous cohort of GIST and revealed marked differences among molecular subgroups. Unlike previous studies that relied on targeted or low-resolution techniques, our method enables systematic, scalable, and genome-wide evaluation of allelic imbalance, thereby providing a new layer of molecular characterization in GIST.

Our results confirm that LOH is a frequent event in GIST, with chromosome 14 emerging as the most commonly affected, consistent with previous reports. Importantly, LOH patterns were not uniformly distributed across samples. Instead, each molecular subgroup displayed a characteristic LOH profile, underscoring the biological heterogeneity of GIST beyond driver mutations (Figure 4).

In particular, *KIT*-mutant GIST exhibited the highest overall burden of chromosomal LOH, suggesting a greater degree of genomic instability in this subgroup. In contrast, *PDGFRA*-mutant GIST showed a lower frequency of chromosomal alterations, consistent with their generally more indolent clinical behavior[18].

SDH-*deficient* GIST displayed the most stable genomic profiles, with LOH restricted to a limited number of chromosomes. This finding aligns with the distinct biology of SDH-*deficient* tumors, which are driven primarily by metabolic and epigenetic dysregulation rather than widespread chromosomal instability. Instead, *NF1*-mutant GISTs were characterized by a strikingly recurrent involvement of chromosome 17, affecting either the p or q arm in a mutually exclusive manner. This observation is consistent with previous reports describing LOH of the *NF1* locus as a secondary hit in NF1-driven GIST tumorigenesis and supports a role for allelic imbalance in disease development[19]. qWT GIST showed marked heterogeneity in LOH patterns: most cases exhibited limited chromosomal involvement, whereas a single case showed extensive genomic instability. This variability likely reflects the biological diversity of this rare subgroup and highlights the diagnostic and biological challenges associated with this rare subset of GIST.

Several chromosomal regions recurrently affected by LOH in our cohort harbor genes with potential relevance to GIST biology. Loss of chromosome arm 1p, observed in 43% of cases, has been previously associated with copy number loss of ENO1, as reported by Assamaki et al[5]. ENO1 is functionally linked to the MYC oncogenic network and has been implicated in tumor metabolism and proliferation in multiple malignancies, including renal, pancreatic, and cervical carcinomas[20-22]. Although the functional interaction between ENO1 and MYC has not yet been explored in GIST, our findings suggest that LOH affecting this region may contribute to deregulation of oncogenic pathways, but this may be the subject of further studies. Moreover, within the 1p36 region, we have previously identified several tumor suppressor genes, including KIF1B, UBE4B, DNAJC11,

PRDM2, and TP73, significantly underexpressed in GISTs, likely as a consequence of chromosomal arm deletion events[6].

Chromosome 14 emerged as the most frequently altered chromosome in our series (63% of cases), consistent with previous reports[5-7]. Multiple genes mapped to 14q11.2 and 14q32.33, including PARP2, APEX1, NDRG2, and SIVA, have been shown to exhibit reduced expression in GIST due to chromosomal deletions[7]. These genes are involved in DNA repair, apoptosis regulation, and cell proliferation, suggesting that LOH affecting chromosome 14 may represent an early and biologically relevant event in GIST pathogenesis, but this needs to be confirmed by specific studies. In addition, YLPM1, a gene located at 14q24 and implicated in telomere maintenance, has been reported to harbor copy-number variations in up to 61% of GIST cases, predominantly due to deletions, further supporting the role of chromosome 14 instability as an early pathogenic event[9].

In our cohort, chromosome 17 alterations were observed in almost all *NF1*-mutant GISTs, affecting 86% of cases, only one KIT-mutant GIST and one SDH-deficient GIST were affected by alterations in chromosome 17. LOH involved either the p or the q arm in a mutually exclusive manner. Alterations *NF1* locus, consistent with previous reports, describing LOH of *NF1* as a secondary hit in *NF1*-driven GIST tumorigenesis[19]. Notably, our analysis indicates that LOH extends across the entire chromosome arm, suggesting a broad allelic imbalance rather than focal loss.

Finally, LOH involving chromosome 22 was detected in 45% of cases, an alteration previously identified in GISTs[23]. This chromosome harbors the tumor suppressor gene NF2, which has been reported as deregulated in GIST and associated with more aggressive tumor behavior[7]. Loss of NF2 function may therefore contribute to disease progression in a subset of GIST, further underscoring the biological relevance of chromosome 22 alterations.

Subgroup-specific LOH patterns revealed by our analysis further reinforce the concept that each molecular subset of GIST has a distinct biological background.

Several studies have reported associations between specific LOH patterns in GISTs and treatment response, suggesting that the significance of LOH events may extend beyond their diagnostic utility[16,24-26]. However, the relatively small size of our cohort, particularly within individual molecular subgroups, limits the ability to perform robust statistical correlations with clinical outcome and to more precisely define the clinical utility of LOH analysis. In particular, within *KIT*-mutant GIST, which exhibits the highest overall burden of chromosomal LOH, the prognostic significance of LOH patterns warrants further investigation.

Moreover, the SNP-based approach used here does not distinguish between LOH associated with copy number losses (CNL-LOH) and LOH associated with copy number gain (CNG-LOH).

Future studies involving larger, independent cohorts will be essential to validate subgroup-specific LOH patterns and to further explore their clinical relevance, including their potential incorporation as prognostic tools. Moreover, integrating SNP-based LOH profiling with transcriptomic and epigenetic data may help clarify the functional impact of recurrent chromosomal alterations and identify novel pathogenic mechanisms in GIST that could represent potential therapeutic targets.

Routine molecular pathology analyses include targeted NGS panels that can inform on CNV of selected genes, but fail to detect LOH and to convey a genome wide molecular cytogenetic analysis. Conversely, SNP-arrays or array-CGH are less frequently used on routine diagnostic procedures due to high costs and time-consuming experimental procedures, other than to technical issues due to formalin artifact in FFPE routine specimens. The approach proposed in this study brings together the rapid turnaround, cost-effectiveness and FFPE compatibility of NGS panel testing with the genome-wide analytical coverage of SNP arrays, thus offering an easy and straightforward assay for routine genome-wide assessment of solid tumors. Moreover, this NGS panel can be run together with other NGS-panel allowing a wide genomic characterization of the SNP sample in the same NGS run, and starting from the same genomic material.

In conclusion, genome-wide SNP-based LOH profiling identifies distinct subgroup-specific patterns of chromosomal imbalance in GIST, supporting its potential value as a complementary tool for molecular characterization alongside driver mutation analysis. Further studies are needed to clarify the clinicopathologic and clinical relevance of these findings.

Author Contributions

T.M., M.N., A.A, M.A.P and D.d.B. provided study concept and design; M.G.P. and A.D.L. provided selection of cases; A.A., T.M., L.G., A.C., D.d.B provided analysis, and interpretation of data; T.M., M.N., A.A. and D.d.B. drafted the manuscript; M.A.P. was involved in critical revision of the manuscript for important intellectual content; M.N. obtained funding. All authors read and approved the final paper.

Data Availability Statement

The datasets used and/or analysed during the current study available from the corresponding author on reasonable request.

Funding

This research was funded by the Italian Ministry of Health, grant number RC-2025-2796962.

Declaration of Competing Interest

The authors declare that the research was conducted in the absence of any commercial or financial relationships that could be construed as a potential conflict of interest.

Ethics Approval and Consent to Participate

The study was performed in accordance with the Declaration of Helsinki protocols. The study was reviewed and approved by the local Institutional Ethical Committee of Azienda Ospedaliero-Universitaria Policlinico S. Orsola-Malpighi, Bologna, Italy (approval number 113/2008/U/Tess), and informed consent was provided by all living patients.

References

1. D'Ambrosio, L., Sbaraglia, M., Merlini, A., Rabino, M., Grignani, G., Appolloni, V., Badalamenti, G., Baldi, G.G., Bellan, E., Benelli, M., et al. (2025). Extended molecular profiling in mesenchymal tumors: a consensus paper from the Italian Sarcoma Group. Crit Rev Oncol Hematol, 104960. 10.1016/j.critrevonc.2025.104960.
2. Pantaleo, M.A., Urbini, M., Indio, V., Ravegnini, G., Nannini, M., De Luca, M., Tarantino, G., Angelini, S., Gronchi, A., Vincenzi, B., et al. (2017). Genome-Wide Analysis Identifies MEN1 and MAX Mutations and a Neuroendocrine-Like Molecular Heterogeneity in Quadruple WT GIST. Mol Cancer Res *15*, 553-562. 10.1158/1541-7786.MCR-16-0376.
3. Patil, D.T., and Rubin, B.P. (2015). Genetics of Gastrointestinal Stromal Tumors: A Heterogeneous Family of Tumors? Surg Pathol Clin *8*, 515-524. 10.1016/j.path.2015.05.006.
4. Nannini, M., Astolfi, A., Urbini, M., Indio, V., Santini, D., Heinrich, M.C., Corless, C.L., Ceccarelli, C., Saponara, M., Mandrioli, A., et al. (2014). Integrated genomic study of quadruple-WT GIST (KIT/PDGFRA/SDH/RAS pathway wild-type GIST). BMC Cancer *14*, 685. 10.1186/1471-2407-14-685.
5. Assamaki, R., Sarlomo-Rikala, M., Lopez-Guerrero, J.A., Lasota, J., Andersson, L.C., Llombart-Bosch, A., Miettinen, M., and Knuutila, S. (2007). Array comparative genomic hybridization analysis of chromosomal imbalances and their target genes in gastrointestinal stromal tumors. Genes Chromosomes Cancer *46*, 564-576. 10.1002/gcc.20439.
6. Astolfi, A., Nannini, M., Pantaleo, M.A., Di Battista, M., Heinrich, M.C., Santini, D., Catena, F., Corless, C.L., Maleddu, A., Saponara, M., et al. (2010). A molecular portrait of gastrointestinal stromal tumors: an integrative analysis of gene expression profiling and high-resolution genomic copy number. Lab Invest *90*, 1285-1294. 10.1038/labinvest.2010.110.
7. Fukasawa, T., Chong, J.M., Sakurai, S., Koshiishi, N., Ikeno, R., Tanaka, A., Matsumoto, Y., Hayashi, Y., Koike, M., and Fukayama, M. (2000). Allelic loss of 14q and 22q, NF2 mutation, and genetic instability occur independently of c-kit mutation in gastrointestinal stromal tumor. Jpn J Cancer Res *91*, 1241-1249. 10.1111/j.1349-7006.2000.tb00910.x.
8. Faucz, F.R., Horvath, A.D., Assie, G., Almeida, M.Q., Szarek, E., Boikos, S., Angelousi, A., Levy, I., Maria, A.G., Chitnis, A., et al. (2023). Embryonic stem cell factor FOXD3 (Genesis) defects in gastrointestinal stromal tumors. Endocr Relat Cancer *30*. 10.1530/ERC-23-0067.
9. Xie, F., Luo, S., Liu, D., Lu, X., Wang, M., Liu, X., Jia, F., Pang, Y., Shen, Y., Zeng, C., et al. (2024). Genomic and transcriptomic landscape of human gastrointestinal stromal tumors. Nat Commun *15*, 9495. 10.1038/s41467-024-53821-1.
10. Zhang, X., and Sjoblom, T. (2021). Targeting Loss of Heterozygosity: A Novel Paradigm for Cancer Therapy. Pharmaceuticals (Basel) *14*. 10.3390/ph14010057.
11. de Biase, D., Acquaviva, G., Visani, M., Marucci, G., De Leo, A., Maloberti, T., Sanza, V., Di Oto, E., Franceschi, E., Mura, A., et al. (2021). Next-Generation Sequencing Panel for 1p/19q Codeletion and IDH1-IDH2 Mutational Analysis Uncovers Mistaken Overdiagnoses of 1p/19q Codeletion by FISH. J Mol Diagn *23*, 1185-1194. 10.1016/j.jmoldx.2021.06.004.
12. Geng, J., Wang, X., Zhao, L., Zhang, J., and Niu, H. (2024). Segmental chromosome aberrations as a prognostic factor of neuroblastoma: a meta-analysis and systematic review. Transl Pediatr *13*, 1789-1798. 10.21037/tp-24-200.
13. Pepe, F., Guerini-Rocco, E., Fassan, M., Fusco, N., Vacirca, D., Ranghiero, A., Venetis, K., Rappa, A., Taormina, S.V., Russo, G., et al. (2024). In-house homologous recombination deficiency testing in ovarian cancer: a multi-institutional Italian pilot study. J Clin Pathol *77*, 478-485. 10.1136/jcp-2023-208852.
14. Nannini, M., Astolfi, A., Maloberti, T., Nigro, M.C., Gozzellino, L., Costa, A., Pirini, M.G., De Leo, A., Grillini, M., Altimari, A., et al. (2025). Performance and clinical utility of two targeted multigene panels for GIST molecular characterization. Sci Rep *16*, 855. 10.1038/s41598-025-30548-7.

15. Urbini, M., Astolfi, A., Indio, V., Heinrich, M.C., Corless, C.L., Nannini, M., Ravegnini, G., Biasco, G., and Pantaleo, M.A. (2015). SDHC methylation in gastrointestinal stromal tumors (GIST): a case report. BMC Med Genet *16*, 87. 10.1186/s12881-015-0233-7.
16. Ylipaa, A., Hunt, K.K., Yang, J., Lazar, A.J., Torres, K.E., Lev, D.C., Nykter, M., Pollock, R.E., Trent, J., and Zhang, W. (2011). Integrative genomic characterization and a genomic staging system for gastrointestinal stromal tumors. Cancer *117*, 380-389. 10.1002/cncr.25594.
17. Gorunova, L., Boye, K., Panagopoulos, I., Berner, J.M., Bjerkehagen, B., Hompland, I., Lobmaier, I., Holmebakk, T., Hveem, T.S., Heim, S., and Micci, F. (2022). Cytogenetic and molecular analyses of 291 gastrointestinal stromal tumors: site-specific cytogenetic evolution as evidence of pathogenetic heterogeneity. Oncotarget *13*, 508-517. 10.18632/oncotarget.28209.
18. Rizzo, A., Pantaleo, M.A., Astolfi, A., Indio, V., and Nannini, M. (2021). The Identity of PDGFRA D842V-Mutant Gastrointestinal Stromal Tumors (GIST). Cancers (Basel) *13*. 10.3390/cancers13040705.
19. Stewart, D.R., Corless, C.L., Rubin, B.P., Heinrich, M.C., Messiaen, L.M., Kessler, L.J., Zhang, P.J., and Brooks, D.G. (2007). Mitotic recombination as evidence of alternative pathogenesis of gastrointestinal stromal tumours in neurofibromatosis type 1. J Med Genet *44*, e61. 10.1136/jmg.2006.043075.
20. Dang, T., You, Y., Wei, L., Li, Q., Sun, H., Sun, M., Li, X., Yang, S., Zeng, T., Zhang, L., et al. (2025). ICAT drives lactylation of tumor-associated macrophages via the c-Myc-ENO1 axis to promote cervical cancer progression. Free Radic Biol Med *241*, 316-329. 10.1016/j.freeradbiomed.2025.09.031.
21. Lu, Y., Ma, H., Xiong, X., Du, Y., Liu, L., Wang, J., and Zhao, W. (2025). Deletion of ENO1 sensitizes pancreatic cancer cells to gemcitabine via MYC/RRM1-mediated glycolysis. Sci Rep *15*, 9941. 10.1038/s41598-025-94319-0.
22. Shroff, E.H., Eberlin, L.S., Dang, V.M., Gouw, A.M., Gabay, M., Adam, S.J., Bellovin, D.I., Tran, P.T., Philbrick, W.M., Garcia-Ocana, A., et al. (2015). MYC oncogene overexpression drives renal cell carcinoma in a mouse model through glutamine metabolism. Proc Natl Acad Sci U S A *112*, 6539-6544. 10.1073/pnas.1507228112.
23. Meza-Zepeda, L.A., Kresse, S.H., Barragan-Polania, A.H., Bjerkehagen, B., Ohnstad, H.O., Namlos, H.M., Wang, J., Kristiansen, B.E., and Myklebost, O. (2006). Array comparative genomic hybridization reveals distinct DNA copy number differences between gastrointestinal stromal tumors and leiomyosarcomas. Cancer Res *66*, 8984-8993. 10.1158/0008-5472.CAN-06-1972.
24. Dermawan, J.K., Kelly, C., Gao, Z., Smith, S., Jadeja, B., Singer, S., Tap, W.D., Chi, P., and Antonescu, C.R. (2023). Novel Genomic Risk Stratification Model for Primary Gastrointestinal Stromal Tumors (GIST) in the Adjuvant Therapy Era. Clin Cancer Res *29*, 3974-3985. 10.1158/1078-0432.CCR-23-1184.
25. Silva, M., Veiga, I., Ribeiro, F.R., Vieira, J., Pinto, C., Pinheiro, M., Mesquita, B., Santos, C., Soares, M., Dinis, J., et al. (2010). Chromosome copy number changes carry prognostic information independent of KIT/PDGFRA point mutations in gastrointestinal stromal tumors. BMC Med *8*, 26. 10.1186/1741-7015-8-26.
26. Lee, E.J., Kang, G., Kang, S.W., Jang, K.T., Lee, J., Park, J.O., Park, C.K., Sohn, T.S., Kim, S., and Kim, K.M. (2013). GSTT1 copy number gain and ZNF overexpression are predictors of poor response to imatinib in gastrointestinal stromal tumors. PLoS One *8*, e77219. 10.1371/journal.pone.0077219.

Figure Legends

Figure 1. SNP graphic representation. (A) Chromosome graph without SNPs affected by LOH; (B) Chromosome graph with SNPs affected by LOH; (C) Total chromosome graph represents all SNPs analyzed.

Figure 2. (A) List of cases divided by molecular alteration and related altered chromosomes. The red squares represent chromosomes with LOH throughout their entirety, while the yellow squares represent chromosomes with partial LOH, meaning in only one chromosome arm. The arm with LOH is indicated within the yellow squares. *SDH*: SDH deficient.* (B) Cases divided by molecular alteration and related altered chromosomes.

Figure 3. Distribution of the number of chromosomes affected by loss of heterozygosity (LOH) across tumor samples stratified according to molecular subtype (KIT, PDGFRA, NF1, SDH-deficient, and quadruple wild-type). (A) LOH events involving a single chromosomal arm; (B) LOH events involving entire chromosomes; (C) LOH events involving a single chromosomal arm and entire chromosomes. Each point represents an individual tumor sample. Statistical comparisons were performed using the Kruskal–Wallis test.
qwT: quadruple wild-type, SDH*: SDH-deficient, * p value <0.05, ** p value < 0.01, *** p value <0.001, **** p value < 0.0001.

Figure 4. Chromosomes affected by LOH in different molecular groups in more than 20% of cases.

	KIT	***PDGFRA***	***SDH***	***NF1***	**qWT**
N° (%)	19 (39%) 17 - exon 11 2 - exon 9	9 (18%) 6 – exon 18 (D842V) 3 - exon 18 (non D842V)	8 (16%) 6 – SDHA 2 – SDHC met	7 (14%)	6 (12%)
Gender					
F	9	5	5	6	1
M	10	4	3	1	5
Tumor site					
stomach	6	9	8	-	1
duodenum	2	-	-	-	1
jejunum	3	-	-	7	1
ileum	7	-	-	-	3
rectum	1	-	-	-	-
Risk class					
Null	-	3	-	1	2
Very low	1	3	2	-	-
Low	4	2	1	2	1
Intermediate	5	-	1	2	2
High	8	-	4	1	-
NV	1	1	-	1	1
Disease status					
Localized	17	9	8	7	6
Advanced	2	-	-	-	-

Table 1 Clinic-pathological characteristics of patients included in the study

A

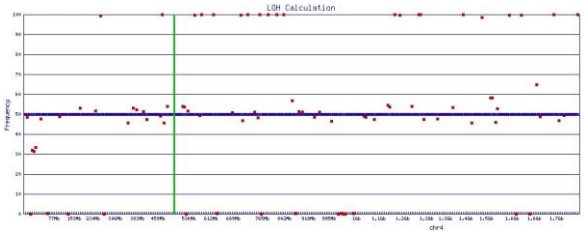

B

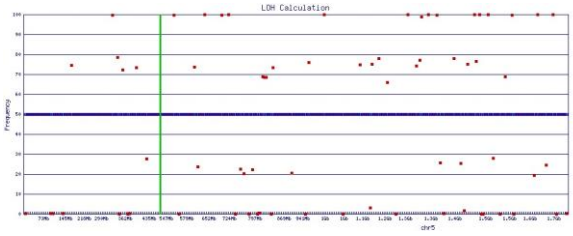

C

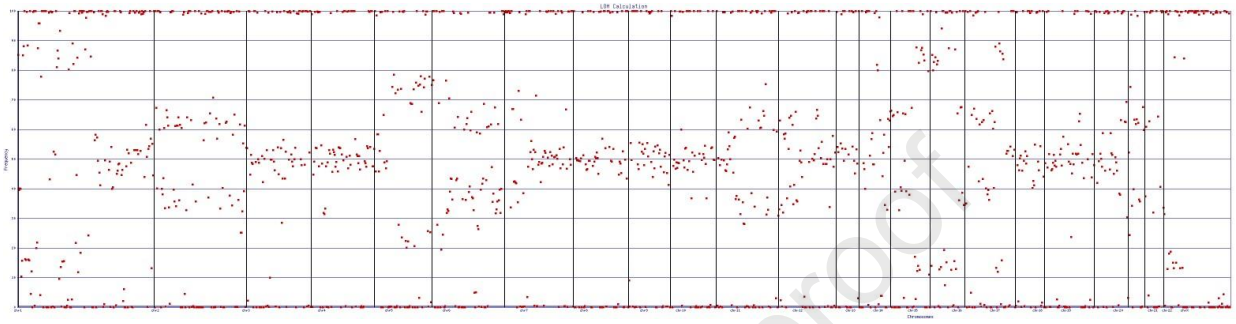

A

Alteration	Cases	1	2	3	4	5	6	7	8	9	10	11	12	13	14	15	16	17	18	19	20	21	22	X	n° chr with total LOH	n° chr with partial LOH
KIT	*1*	q		q													q			q					4	4
	2	p				q	p	q							p										11	5
	3																								2	0
	4	p																							3	1
	5	p																							11	1
	6																								3	0
	7	p																							3	1
	8	p	p																	q					4	3
	9																								1	0
	10	p											q												6	2
	11																				q				4	1
	12																								6	0
	13	p																							2	1
	14	p				q																			4	2
	15	p	q																						5	2
	16	p																p							10	2
	17	p																							3	1
	18	p															p			p					3	3
	19																								2	0
PDGFRα	*20*																								2	0
	21	p																							2	1
	22																								1	0
	23										p														1	1
	24																								0	0
	25						q																		3	1
	26	q																							2	1
	27	p																	p						2	2
	28																				p				1	1
SDH*	*29*																								0	0
	30																								0	0
	31																								0	0
	32																								0	0
	33																								1	0
	34	p										q						p							1	3
	35	p									q								p					q	2	4
	36																								0	0
NF1	*37*	p										p													2	2
	38	p																q							7	2
	39	p									p	p						q							1	4
	40						q											p							7	2
	41				p						q							q							0	3
	42	p				p						p						p							3	4
	43																	p						p	3	2
qWT	*44*																q								3	1
	45																								1	0
	46																			q					18	1
	47	p																							1	1
	48																								0	0
	49																								0	0

B